Journal of Reinforced Plastics and Composites
http://jrp.sagepub.com

Large Deflection Elastic and Inelastic Transient Analyses of Composite and Sandwich Plates with a Refined Theory

J.R. Kommineni and T. Kant

Journal of Reinforced Plastics and Composites 1993; 12; 1150
DOI: 10.1177/073168449301201102

Large Deflection Elastic and Inelastic Transient Analyses of Composite and Sandwich Plates with a Refined Theory

J. R. KOMMINENI* AND T. KANT**
Department of Civil Engineering
Indian Institute of Technology
Powai, Bombay–400 076, India

ABSTRACT: A C° continuous finite element formulation of a higher order displacement theory is presented for predicting linear and non-linear transient responses of composite and sandwich plates. The geometric non-linearity is accounted for in the sense of von Karman assumptions and the material behaviour is assumed as elasto-perfectly plastic. The elasto-perfectly plastic material behaviour is incorporated using the flow theory of plasticity. In particular, the modified version of Hill's initial yield criterion with anisotropic parameters of plasticity is used. The layered approach is adopted to account for the plasticity through the thickness of the plate. The displacement model accounts for non-linear cubic variation of tangential displacement components through the thickness of the laminate and the theory requires no shear correction coefficients. In the time domain, the explicit central difference integrator is used in conjunction with the special mass matrix diagonalization scheme which conserves the total mass of the element and includes effects due to rotary inertia terms. The parametric effects of the time step, finite element mesh, lamination scheme and orthotropy on the linear and non-linear responses are investigated. Numerical results are presented for composite and sandwich plates under various boundary conditions and loadings and these are compared with the results from other sources. Some new results are also presented for future reference.

1. INTRODUCTION

IN RECENT YEARS, because of the increased use of composite materials in the aerospace and automotive industries due to their superior mechanical properties, such as high stiffness per unit weight, high strength per unit weight, and potentially low unit cost, a need has arisen for a basic understanding of their response to dynamic loading.

To the authors' knowledge, investigations predicting the dynamic non-linear transient response of composite and sandwich plates are scarce. A higher order shear deformation theory is utilized here (Kant and Kommineni, 1992a). A C° nine-node bi-quadratic Lagrangian finite element is used together with either full

*Presently at University of Kentucky, Lexington, KY.
**Professor and author to whom correspondence should be addressed.

0731-6844/93/11 1150–21 $6.00/0

integration or uniformly reduced integration techniques for numerical computations. In addition to the higher order shear deformation theory, a formulation for a first order shear deformation theory with five degrees of freedom per node is also developed so as to enable the comparison of present formulation with a parallel formulation both for composite and sandwich plates. Several examples drawn from the literature are analyzed and appropriate comparisons are made to show the simplicity, validity and accuracy of the present formulation.

2. A NON-LINEAR HIGHER ORDER THEORY OF ANISOTROPIC PLATES

A composite laminate consisting of laminas with isotropic/orthotropic material properties oriented arbitrarily is considered. The x–y plane coincides with the middle plane of the laminate with z axis oriented in the thickness direction such that x, y, and z form a right-handed screw coordinate system. The displacement components of a generic point in the laminate are assumed to be of the form:

$$\begin{aligned} u(x,y,z,t) &= u_o(x,y,t) + z\theta_x(x,y,t) + z^2u_o^*(x,y,t) + z^3\theta_x^*(x,y,t) \\ v(x,y,z,t) &= v_o(x,y,t) + z\theta_y(x,y,t) + z^2v_o^*(x,y,t) + z^3\theta_y^*(x,y,t) \\ w(x,y,z,t) &= w_o(x,y,t) \end{aligned} \tag{1}$$

where t denotes the time; u_o, v_o, and w_o are the components of mid-plane displacements of a generic point having displacements u, v, and w in x, y, and z directions, respectively. The other parameters are defined in Kant and Kommineni (1992b, 1992c). Large displacements in the sense of von Karman assumptions are considered here. Both isotropic and anisotropic situations can be accommodated with arbitrary thicknesses for different layers. By invoking von Karman's large deflection assumptions which in particular imply that the first derivatives of u, v, and w with respect to x, y, and z are small, so that their particular products can be neglected (see Pica and Hinton, 1980; Reddy, 1983), the following Green-Lagrangian strain displacement relations are obtained,

$$\begin{aligned} \epsilon_x &= \frac{\partial u}{\partial x} + \frac{1}{2}\left(\frac{\partial w}{\partial x}\right)^2 \\ \epsilon_y &= \frac{\partial v}{\partial y} + \frac{1}{2}\left(\frac{\partial w}{\partial y}\right)^2 \\ \gamma_{xy} &= \frac{\partial u}{\partial y} + \frac{\partial v}{\partial x} + \frac{\partial w}{\partial x}\frac{\partial w}{\partial y} \\ \gamma_{zx} &= \frac{\partial u}{\partial z} + \frac{\partial w}{\partial x} \\ \gamma_{yz} &= \frac{\partial v}{\partial z} + \frac{\partial w}{\partial y} \end{aligned} \tag{2}$$

The equations of motion of the composite and sandwich laminate are developed by using Hamilton's variational principle. The first variation of the Lagrangian function is thus made to vanish such that:

$$\delta \int_{t_1}^{t_2} L_f \, dt = 0 \tag{3}$$

in which $L_f = (\Pi - E)$ and δ is variation taken during indicated time interval and integral of L_f takes an extreme value that can be shown to be a minimum. The parameters E and Π define the kinetic and potential energies of the system, respectively.

The potential energy Π of the system can be written as

$$\begin{aligned} \Pi &= U - W \\ &= \frac{1}{2} \int_V \boldsymbol{\epsilon}^t \boldsymbol{\sigma} dv - \int_V \mathbf{u}^t \mathbf{F} dv - \int_S \mathbf{u}^t \mathbf{T}^* ds \end{aligned} \tag{4a}$$

where U is internal strain energy; W is the work done by the applied loads when displacement varies; the vector $\mathbf{u}$ represents three displacement components u, v, w of a point; the external forces $\mathbf{F}$ and $\mathbf{T}^*$ are body force and surface traction vectors, respectively; and S is the portion of the body on which the tractions are prescribed.

The kinetic energy of the body E can be written as:

$$\mathrm{E} = \frac{1}{2} \int_V \dot{\mathbf{u}}^t \varrho \dot{\mathbf{u}} \, dv \tag{4b}$$

where ϱ is the mass density of the material and $\dot{\mathbf{u}}$ defines the particle velocity vector. Rewriting Equation (3), we have

$$\delta \int_{t_1}^{t_2} \left(\frac{1}{2} \int_V \boldsymbol{\epsilon}^t \boldsymbol{\sigma} \, dv - \int_V \mathbf{u}^t \mathbf{F} \, dv - \int_S \mathbf{u}^t \mathbf{T}^* \, ds - \frac{1}{2} \int_V \dot{\mathbf{u}}^t \varrho \dot{\mathbf{u}} dv \right) dt = 0 \tag{5}$$

Substitution of the expressions for strain components in Equation (5) and an explicit integration through the laminate thickness lead to the definition of a stress resultant vector, $\bar{\boldsymbol{\sigma}}$, which is defined as follows:

$$\begin{aligned} \bar{\boldsymbol{\sigma}} = (&N_x, N_y, N_{xy}, Q_x, Q_y, M_x, M_y, M_{xy}, S_x, S_y, \\ &N_x^*, N_y^*, N_{xy}^*, Q_x^*, Q_y^*, M_x^*, M_y^*, M_{xy}^*)^t \end{aligned} \tag{6a}$$

The individual components are approximated as:

$$\begin{bmatrix} N_x & M_x & N_x^* & M_x^* \\ N_y & M_y & N_y^* & M_y^* \\ N_{xy} & M_{xy} & N_{xy}^* & M_{xy}^* \\ Q_x & S_x & Q_x^* & - \\ Q_y & S_y & Q_y^* & - \end{bmatrix} = \sum_{L=1}^{NL} \begin{bmatrix} \sigma_x \\ \sigma_y \\ \tau_{xy} \\ \tau_{xz} \\ \tau_{yz} \end{bmatrix} [1 \quad \bar{z} \quad \bar{z}^2 \quad \bar{z}^3] \quad [z^{L+1} - z^L] \tag{6b}$$

where $\sigma^t = [\sigma_x, \sigma_y, \tau_{xy}, \tau_{xz}, \tau_{yz}]$ and $\epsilon^t = [\epsilon_x, \epsilon_y, \gamma_{xy}, \gamma_{xz}, \gamma_{yz}]$ are, respectively, vectors of stress and strain components with respect to laminate axes (see Figure 1) and $\bar{z} = (z^{L+1}+z^L)/2$. The reader is urged to refer to Kommineni and Kant (1993) for the details of incremental stress-strain relations.

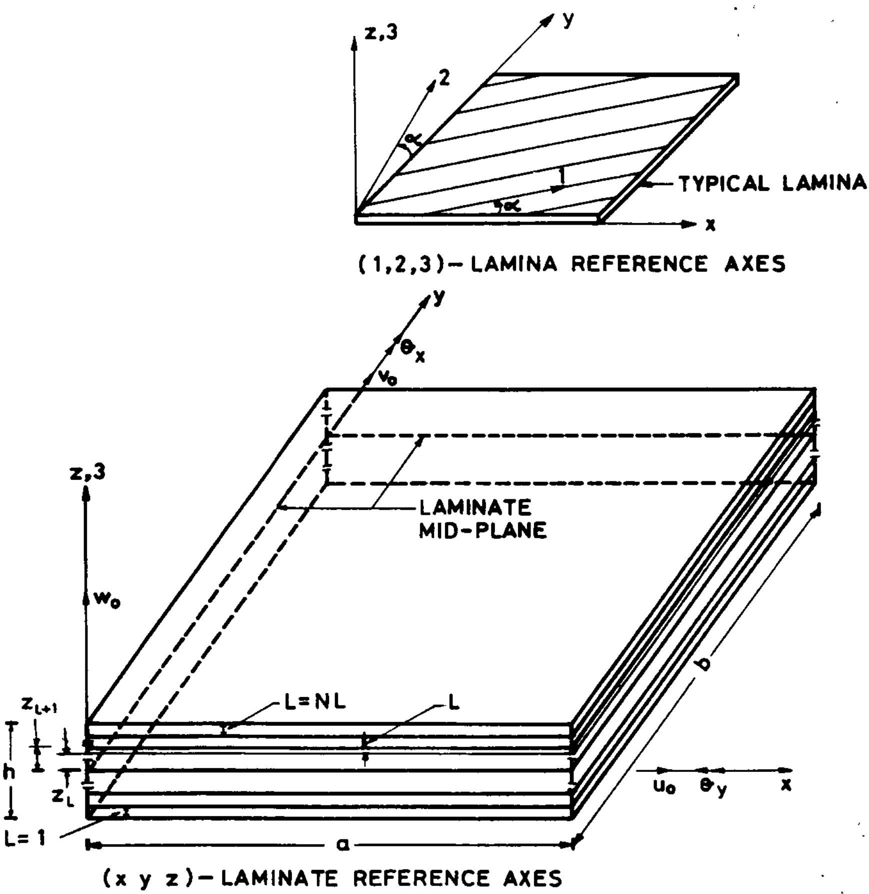

***Figure 1.** Laminated plate geometry with positive set of lamina/laminate reference axes, displacement components and fibre orientation.*

The two-dimensional laminate constitutive equations are written in a matrix form as follows:

$$\begin{bmatrix} \mathbf{N} \\ \mathbf{M} \\ \mathbf{N}^* \\ \mathbf{M}^* \end{bmatrix} = \begin{bmatrix} \mathbf{D}_0 & \mathbf{D}_1 & \mathbf{D}_2 & \mathbf{D}_3 \\ & \mathbf{D}_2 & \mathbf{D}_3 & \mathbf{D}_4 \\ & & \mathbf{D}_4 & \mathbf{D}_5 \\ \text{symmetric} & & & \mathbf{D}_6 \end{bmatrix} \begin{bmatrix} \boldsymbol{\epsilon}_o \\ \mathbf{k} \\ \boldsymbol{\epsilon}_o^* \\ \mathbf{k}^* \end{bmatrix} \tag{7a}$$

where

$$\begin{aligned} \mathbf{N} &= [N_x, N_y, N_{xy}, Q_x, Q_y]^t \ ; \quad \mathbf{M} = [M_x, M_y, M_{xy}, S_x, S_y]^t \\ \mathbf{N}^* &= [N_x^*, N_y^*, N_{xy}^*, Q_x^*, Q_y^*]^t \ ; \ \mathbf{M}^* = [M_x^*, M_y^*, M_{xy}^*, 0, 0]^t \\ \boldsymbol{\epsilon}_o &= [\epsilon_{xo}, \epsilon_{yo}, \epsilon_{xyo}, \phi_x, \phi_y]^t \ ; \quad \mathbf{k} = [k_x, k_y, k_{xy}, \varkappa_x, \varkappa_y]^t \\ \boldsymbol{\epsilon}_o^* &= [\epsilon_{xo}^*, \epsilon_{yo}^*, \epsilon_{xyo}^*, \phi_x^*, \phi_y^*]^t \ ; \quad \mathbf{k}^* = [k_x^*, k_y^*, k_{xy}^*, 0, 0]^t \end{aligned} \tag{7b}$$

and

$$\mathbf{D}_i = \sum_{L=1}^{NL} \begin{bmatrix} Q_{11}C\bar{z}^i & Q_{12}C\bar{z}^i & Q_{13}C\bar{z}^i & Q_{14}C\bar{z}^i & Q_{15}C\bar{z}^i \\ & Q_{22}C\bar{z}^i & Q_{23}C\bar{z}^i & Q_{24}C\bar{z}^i & Q_{25}C\bar{z}^i \\ & & Q_{33}C\bar{z}^i & Q_{34}C\bar{z}^i & Q_{35}C\bar{z}^i \\ & & & Q_{44}C\bar{z}^i & Q_{45}C\bar{z}^i \\ \text{symmetric} & & & & Q_{55}C\bar{z}^i \end{bmatrix} \tag{7c}$$

where

$$C = (z^{L+1} - z^L) \quad \text{and} \quad \bar{z}^i = \left(\frac{z^{L+1} + z^L}{2}\right)^i \tag{7d}$$

The mid-plane strain vectors $\bar{\epsilon}$, $\bar{\mathbf{k}}$, $\bar{\epsilon}^*$, and $\bar{\mathbf{k}}^*$ are defined as follows,

$$\bar{\epsilon} = \begin{bmatrix} \dfrac{\partial u_o}{\partial x} + \dfrac{1}{2}\left(\dfrac{\partial w_o}{\partial x}\right)^2 \\ \dfrac{\partial v_o}{\partial y} + \dfrac{1}{2}\left(\dfrac{\partial w_o}{\partial y}\right)^2 \\ \dfrac{\partial v_o}{\partial x} + \dfrac{\partial u_o}{\partial y} + \dfrac{\partial w_o}{\partial x}\dfrac{\partial w_o}{\partial y} \\ \theta_x + \dfrac{\partial w_o}{\partial x} \\ \theta_y + \dfrac{\partial w_o}{\partial y} \end{bmatrix}; \ \bar{\mathbf{k}} = \begin{bmatrix} \dfrac{\partial \theta_x}{\partial x} \\ \dfrac{\partial \theta_y}{\partial y} \\ \dfrac{\partial \theta_y}{\partial x} + \dfrac{\partial \theta_x}{\partial y} \\ 3\theta_x^* \\ 3\theta_y^* \end{bmatrix};$$

$$\bar{\epsilon}^* = \begin{bmatrix} \dfrac{\partial u_o^*}{\partial x} \\ \dfrac{\partial v_o^*}{\partial y} \\ \dfrac{\partial v_o^*}{\partial x} + \dfrac{\partial u_o^*}{\partial y} \\ 2u_o^* \\ 2v_o^* \end{bmatrix}; \bar{\mathbf{k}}^* = \begin{bmatrix} \dfrac{\partial \theta_x^*}{\partial x} \\ \dfrac{\partial \theta_y^*}{\partial y} \\ \dfrac{\partial \theta_y^*}{\partial x} + \dfrac{\partial \theta_x^*}{\partial y} \\ 0 \\ 0 \end{bmatrix} \quad (8)$$

3. C° FINITE ELEMENT FORMULATION

The finite element used here is a nine-node isoparametric quadrilateral element. The laminate displacement field in the element can be expressed in terms of nodal variables, such that

$$\mathbf{d}(\zeta,\eta) = \sum_{i=1}^{NN} \mathbf{N}_i(\zeta,\eta) \cdot \mathbf{d}_i \quad (9a)$$

or

$$\mathbf{d}(\zeta,\eta) = [\mathbf{N}_1, \mathbf{N}_2, \mathbf{N}_3, \ldots, \mathbf{N}_{NN}] \begin{bmatrix} \mathbf{d}_1 \\ \mathbf{d}_2 \\ \mathbf{d}_3 \\ \vdots \\ \mathbf{d}_{NN} \end{bmatrix} \quad (9b)$$

or

$$\mathbf{d} = \mathbf{Na} \quad (9c)$$

where NN represents the number of nodes in the element; $N_i(\zeta,\eta)$ defines interpolation function associated with node i in terms of normalized coordinates ζ and η; and $\mathbf{d}_i$ is a generalized displacement vector of the mid-plane at node i, such that

$$\mathbf{d}_i^t = (u_{oi}, v_{oi}, w_{oi}, \theta_{xi}, \theta_{yi}, u_{oi}^*, v_{oi}^*, \theta_{xi}^*, \theta_{yi}^*) \quad (10)$$

The generalized vectors of Green strain and its variation $\bar{\epsilon}$ and $\delta\bar{\epsilon}$, respectively are written in terms of nodal displacements, **a**; displacement gradient, and Cartesian derivatives of shape functions as follows:

$$\bar{\epsilon} = \left(\mathbf{B}_o + \frac{1}{2}\mathbf{B}_{nl}\right)\mathbf{a}$$

$$\delta\bar{\epsilon} = (\mathbf{B}_o + \mathbf{B}_{nl})\,\delta\mathbf{a} \tag{11}$$

$$\delta\bar{\sigma} = \mathbf{D}\,\mathbf{B}\,\delta\mathbf{a}$$

where $\mathbf{B}_o$ is the linear strain displacement matrix and $\mathbf{B}_{nl}$ the non-linear strain displacement matrix which is linearly dependent upon the nodal displacement **a.** **B** is the total strain displacement matrix. The linear part of strain can be written as,

$$\bar{\epsilon}_{ol} = \sum_{i=1}^{NN} \mathbf{B}_{pi}\,\mathbf{d}_i = \mathbf{B}_p\,\mathbf{a} \quad ; \quad \mathbf{k} = \sum_{i=1}^{NN} \mathbf{B}_{fi}\mathbf{d}_i = \mathbf{B}_f\,\mathbf{a}$$

$$\bar{\epsilon}^*_{ol} = \sum_{i=1}^{NN} \mathbf{B}_{psi}\,\mathbf{d}_i = \mathbf{B}_{ps}\,\mathbf{a} \;;\; \mathbf{k}^* = \sum_{i=1}^{NN} \mathbf{B}_{fsi}\,\mathbf{d}_i = \mathbf{B}_{fs}\,\mathbf{a} \tag{12}$$

The corresponding non-zero terms of the sub-matrices of $\mathbf{B}_o$ matrix are as follows:

The matrices $\mathbf{B}_p$, $\mathbf{B}_f$, $\mathbf{B}_{ps}$, and $\mathbf{B}_{fs}$ are of dimension 5 × 9.

The non-zero terms of $\mathbf{B}_p$ matrix are:

$$B_{11} = B_{33} = B_{43} = \frac{\partial N_i}{\partial x} \;;\; B_{22} = B_{31} = B_{53} = \frac{\partial N_i}{\partial y} \;;\; B_{44} = B_{55} = N_i$$

The non-zero terms of the $\mathbf{B}_f$ matrix are:

$$B_{14} = B_{35} = \frac{\partial N_i}{\partial x} \;;\; B_{25} = B_{34} = \frac{\partial N_i}{\partial y} \;;\; B_{46} = B_{57} = 2N_i$$

The non-zero terms of $\mathbf{B}_{ps}$ matrix are:

$$B_{16} = B_{37} = \frac{\partial N_i}{\partial x} \;;\; B_{27} = B_{76} = \frac{\partial N_i}{\partial y} \;;\; B_{48} = B_{59} = 3N_i$$

The non-zero terms of $\mathbf{B}_{fs}$ matrix are:

$$B_{18} = B_{39} = \frac{\partial N_i}{\partial x} \;;\; B_{29} = B_{38} = \frac{\partial N_i}{\partial y}$$

The discrete form of the Equation (5) takes the form:

$$\int_{t_1}^{t_2} \delta a^t \left(\mathbf{M}\ddot{\mathbf{a}} + \mathbf{P}(a,t) - \mathbf{F}(t) \right) dt = 0 \tag{13}$$

Because this relation is valid for every virtual displacement $\epsilon\mathbf{a}$, one obtains,

$$\mathbf{M}\ddot{\mathbf{a}} + \mathbf{P}(a,t) = \mathbf{F}(t) \tag{14}$$

which is the global equation of motion, where $\mathbf{M}$ is the global mass matrix; $\mathbf{P}(a,t)$ and $\mathbf{F}(t)$ are, respectively, global internal and external load vectors at time t—they are given in subsequent sections:

$$\mathbf{P}(a,t) = \int_A \mathbf{B}^t \bar{\sigma}\, dx\, dy \tag{15}$$

In material non-linear analysis for the yielded Gaussian point, the stresses are calculated so that the yielding criterion is satisfied. If the actual stress is found greater than this permissible value, then the portion of the stress greater than the yield value must be reduced to the yield surface (see Owen and Hinton, 1980 and Kommineni and Kant, 1993).

4. SPECIAL MASS MATRIX DIAGONALIZATION SCHEME

The inertia force vector requires the evaluation of the mass matrix $\mathbf{M}$. This consistent mass matrix is not diagonal and it must therefore be diagonalized in some way if it is to be useful in the explicit time marching scheme. For the quadratic isoparametric element used here, the following procedure is adopted.

The diagonalized coefficients of the consistent mass matrix are computed

$$\mathbf{M} = \int_A \mathbf{N}^t \bar{\mathbf{m}} \mathbf{N}\, dA \tag{16}$$

$$\text{where } \bar{\mathbf{m}} = \begin{bmatrix} I_1 & & & & & & & & 0 \\ & I_1 & & & & & & & \\ & & I_1 & & & & & & \\ & & & I_2 & & & & & \\ & & & & I_2 & & & & \\ & & & & & I_3 & & & \\ & & & & & & I_3 & & \\ & & & & & & & I_4 & \\ 0 & & & & & & & & I_4 \end{bmatrix}$$

in which I_1, I_2, I_3, I_4 are normal inertia, rotary inertia, and respective higher order inertia terms. These terms are given by

$$(I_1, I_2, I_3, I_4) = \sum_{L=1}^{NL} \int_{z_L}^{z_{L+1}} (1, z^2, z^4, z^6)\, \varrho^L\, dz \tag{17}$$

and ϱ^L is material density of the L^{th} layer.

All the diagonal terms are scaled with respect to the translation (but not rotation) terms in such a way that the total mass of the element is conserved.

5. SOLUTION ALGORITHM

The numerical solution to the ordinary differential Equation (14) is obtained using an explicit central difference scheme. The advantage of using the central difference method should now become apparent. Since no internal force vector and mass matrices of the complete element assemblage need to be calculated, the solution can essentially be carried out on the element level and relatively little high speed storage is required. Further, the usual iterative solution procedure for the solution of a non-linear system of equations is completely avoided since the solution in the time domain is obtained here for each degree of freedom independently. Using the central difference scheme, systems of very large order equations can be solved efficiently. This scheme can be written as,

$$\mathbf{a}^{n+1} = \mathbf{M}^{-1} \times (\Delta t)^2 (-\mathbf{p}^n + \mathbf{F}^n) - a^{n-1} - 2a^n \tag{18}$$

where superscripts $n - 1, n, n + 1$ stand for three successive time stages and Δt is the time step length. The main advantage of this approach is that when $\mathbf{M}$ is diagonal, the computations at each step are trivial.

No estimate on the time step for the non-linear analysis is available in the literature. An initial estimate is calculated here using the modified formula of Tsui and Tong (1971) by Mallikarjuna and Kant (1990):

$$\Delta t \leq \Delta t_{cri} = \Delta x \left(\frac{\varrho(1 - \nu^2)/E_2 R}{\{2 + (1-\nu)(\pi^2/12)(1 + 1.5(\Delta x/h)^2\}} \right)^{1/2} \tag{19}$$

in which Δx is the smallest distance between adjacent nodes in any quadrilateral element used. E_1 and E_2 are the Young's moduli in 1 and 2 directions, respectively (see Figure 1) and $R = E_1/E_2$. The final estimate is done after carrying out the convergence checks in order to save the computational costs.

6. NUMERICAL RESULTS

In the present study, the nine-node quadrilateral isoparametric element is employed. Because of the biaxial symmetry of the problems discussed, only one quadrant of the laminate is analyzed with 2 × 2 mesh, except for angle-ply laminates that are analyzed by considering full laminates with 4 × 4 mesh. In all the numerical computations, either a full integration rule (3 × 3) or an uniformly reduced (2 × 2) integration rule is employed. The element mass matrix is evaluated using a 3 × 3 Gaussian-quadrature rule. In the present layered approach, lamina are divided into 8 to 10 layers, depending on the lamination scheme. For numerical computations two programs are developed—a first order shear deformation theory (FOST) and a higher order shear deformation theory (HOST) with five and nine degrees of freedom per node, respectively. All the computations were carried out in single precision on CDC Cyber 180/840 computer with sixteen significant digits word length at Indian Institute of Technology, Bombay, India. All the stress values are evaluated at the Gaussian points. The shear correction coefficient used in the first order shear deformation theory is assumed as 5/6.

In order to test the accuracy and efficiency of the developed algorithm and to investigate the effects of transverse shear deformations, the following material property sets were used in obtaining the numerical results.

Material set 1: the material properties are taken from Reismann and Lee (1969).

$$a = \sqrt{2}, b = 1, h = 0.2, \varrho = 1, \nu = 0.3 \text{ and } E = 1 \text{ (non-dimensional)}$$

Material set 2: the material properties are taken from Nosier and Reddy (1991).

Middle layer $E = 19.2 \times 10^6$ psi; $\nu = 0.24$; $E_z = 1.56 \times 10^6$ psi
$G_z = 0.82 \times 10^6$ psi; $\nu_z = 0.24$ and $\varrho = 0.00013$ lb s^2/in^4
Outer layers $E = 20.83 \times 10^6$ psi; $\nu = 0.44$; $E_z = 10.0 \times 10^6$ psi
$G_z = 3.7 \times 10^6$ psi; $\nu_z = 0.44$ and $\varrho = 0.00013$ lb s^2/in^4
Geometry $a/h = 10$; $h = 1$; $h_1 = h_3 = h_2/2$

Material set 3: the material properties are taken from Pica and Hinton (1980).

$$E = 100 \text{ psi}; \nu = 0.3; \varrho = 10 \text{ lb s}^2/\text{in}^4,$$
$$a = 10 \text{ in}; b = 1 \text{ in}; h = 1 \text{ in}; q_o = 0.02 \text{ lb/in}^2$$

Material set 4: the material properties are taken from Reddy (1983).

$$E_1 = 25 E_2;\ \nu_{12} = \nu_{23} = \nu_{31} = 0.25;\ G_{12} = G_{31} = 0.5 E_2;\ G_{23} = 0.2 E_2;$$
$$E_2 = 1;\ \varrho = 1.$$

Material set 5: the material properties are taken from Kant (1987).

$$a = b = 100 \text{ cm}, h = 10 \text{ cm}$$

Face sheets (graphite/epoxy prepreg system)

$$E_1 = 1.308 \times 10^7 \text{ N/cm}^2; E_2 = 1.06 \times 10^6 \text{ N/cm}^2;$$
$$G_{12} = G_{13} = 6 \times 10^5 \text{ N/cm}^2,$$
$$G_{23} = 3.9 \times 10^5 \text{ N/cm}^2; \varrho = 1.58 \times 10^{-5} \text{ N s}^2/\text{cm}^4;$$
$$\nu_{12} = \nu_{23} = \nu_{23} = 0.28$$

Thickness of each top stiff layer $= 0.025h$
Thickness of each bottom stiff layer $= 0.08125h$

Core (U.S. commerical aluminum honeycomb)
Thickness of core = $0.6h$

Core 1

$$G_{23} = 1.772 \times 10^4 \,\text{N/cm}^2;\ G_{13} = 5.206 \times 10^4 \,\text{N/cm}^2;$$
$$\varrho = 1.009 \times 10^{-6} \,\text{N s}^2/\text{cm}^4$$

Core 2

$$G_{23} = 1.772 \times 10^2 \,\text{N/cm}^2;\ G_{13} = 5.206 \times 10^2 \,\text{N/cm}^2;$$
$$\varrho = 1.009 \times 10^{-6} \,\text{N s}^2/\text{cm}^4$$

Material set 6: the material properties are taken from Liu and Lin (1979).

$$E_1 = E_2 = 10 \times 10^6 \text{ psi};\ G_{12} = G_{13} = G_{23} = 3.846 \times 10^6 \text{ psi};\ \nu = 0.3$$

Plasticity parameters

$$\sigma_1^o = \sigma_2^o = \sigma_3^o = 3.0 \times 10^4 \text{psi};\ \sigma_{12}^o = \sigma_{13}^o = \sigma_{23}^o = 1.372 \times 10^4 \text{psi};$$
$$\varrho = 0.000259 \text{ lb s}^2/\text{in}^4$$

Material set 7: the material properties are taken from Nanda and Kuppusamy (1991).

$$E_1 = 25\,E_2;\ G_{12} = G_{23} = G_{31} = 0.5\,E_2;\ \varrho = 8 \times 10^{-6} \,\text{N s}^2/\text{cm}^4$$
$$\nu_{12} = \nu_{23} = \nu_{31} = 0.25;\ E_2 = 1.0 \times 10^6 \,\text{N/cm}^2\, a = b = 10\,\text{cm}$$
$$\sigma_1^o = 1.0 \times 10^4 \,\text{N/cm}^2;\ \sigma_2^o = \sigma_3^o = 0.4 \times 10^4 \,\text{N/cm}^2;$$
$$\sigma_{12}^o = \sigma_{13}^o = 0.37 \times 10^4 \,\text{N/cm}^2;\ \sigma_{23}^o = 0.23 \times 10^4 \,\text{N/cm}^2$$

The boundary conditions corresponding to the present higher order formulation are specified in Table 1 for different types of supports used in the present investigation.

The corresponding boundary conditions for the first order shear deformation theory are obtained simply by omitting the higher order starred (*) displacement quantities. For example, there are nine displacement quantities required to be specified at $x = 0,a$ for C type of boundary conditions in this higher order formulation (HOST), whereas in first order formulation (FOST) the corresponding boundary values shall be five only. The boundary condition types S1 and S2 have been especially chosen in order to compare our results with those of other authors. Incidentally, the S1 type condition corresponds to the usual diaphragm type of simple support. The edge conditions, which have been derived in a variationally consistent manner in the present higher order theory may not appear so (except in the case of fully clamped edge specified by C), because, in any way, the natural boundary conditions cannot be prescribed in the displacement based finite element method.

Table 1. Boundary conditions.

Type	x = 0 / x = a		x = a/2		y = 0 / y = b		y = b/2	
S1	$v_o = 0$ $\theta y = 0$ $w_o = 0$	$v_o^* = 0$ $\theta_y^* = 0$	$u_o = 0$ $\theta_x = 0$	$u_o^* = 0$ $\theta_x^* = 0$	$u_o = 0$ $\theta_x = 0$ $w_o = 0$	$u_o^* = 0$ $\theta_x^* = 0$	$v_o = 0$ $\theta_y = 0$	$v_o^* = 0$ $\theta_y^* = 0$
S2	$u_o = 0$ $\theta_y = 0$ $w_o = 0$	$u_o^* = 0$ $\theta_y^* = 0$	$u_o = 0$ $\theta_x = 0$	$u_o^* = 0$ $\theta_x^* = 0$	$v_o = 0$ $\theta_x = 0$ $w_o = 0$	$v_o^* = 0$ $\theta_x^* = 0$	$v_o = 0$ $\theta_y = 0$	$v_o^* = 0$ $\theta_y^* = 0$
C	$u_o = 0$ $v_o = 0$ $\theta_x = 0$ $\theta_y = 0$ $w_o = 0$	$u_o^* = 0$ $v_o^* = 0$ $\theta_x^* = 0$ $\theta_y^* = 0$	$u_o = 0$ $\theta_x = 0$	$u_o^* = 0$ $\theta_x^* = 0$	$u_o = 0$ $v_o = 0$ $\theta_x = 0$ $\theta_y = 0$ $w_o = 0$	$u_o^* = 0$ $v_o^* = 0$ $\theta_x^* = 0$ $\theta_y^* = 0$	$v_o = 0$ $\theta_y = 0$	$v_o^* = 0$ $\theta_y^* = 0$

6.1 Linear Analysis

6.1.1 ISOTROPIC PLATE SUBJECTED TO PATCH LOAD AT THE CENTER

In order to validate the present theory, a problem for which an analytical solution exists has been solved. The problem consists of a simply supported (S1) rectangular plate with geometry and material properties as per material set 1 subjected to an uniform pulse load on a square (side = 0.4b) area at the center of the plate. A non-uniform 4 × 4 mesh of elements was employed. A comparison of non-dimensional center deflection and bending moments obtained by present theory and Reismann and Lee (1969) is shown in Figures 2a and 2b. The classical plate theory results (i.e., not accounting for transverse shear strains) is also given in the figures to show the influence of shear deformation on the results. The present finite element solution for the center deflection is in excellent agreement with a thick plate analytical solution. The non-dimensional quantities used are as follows:

$$\hat{t} = (t/b)(\sqrt{E/\varrho}); \; \hat{w}_o = \left(\frac{w_o E a h}{q_o b^3}\right); \; \hat{M} = \left(\frac{12 a M_y}{q_o b^2 h^2}\right) \tag{20}$$

6.1.2 LAYERED ORTHOTROPIC PLATE

To validate the present theory further, another problem for which a closed-form higher order solution exists has been solved. For this purpose, a three-layer (thickness of each outer layer equals half of the thickness of middle layer) simply supported (S1) orthotropic laminate with geometry and material properties as per material set 2, subjected to a step, a triangular and a symmetric N wave with durations 0.002 sec, 0.001 sec and 0.001 sec, respectively, is considered. The present responses are compared with a closed form higher order solution re-

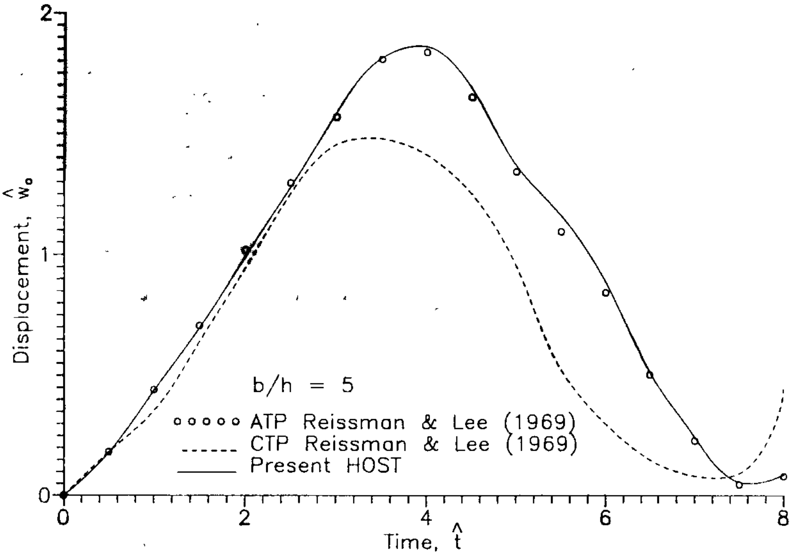

Figure 2a. *Displacement vs. time for a simply supported (S1), rectangular isotropic plate under suddenly applied patch load (q_o = 1, Δt = 0.02 sec).*

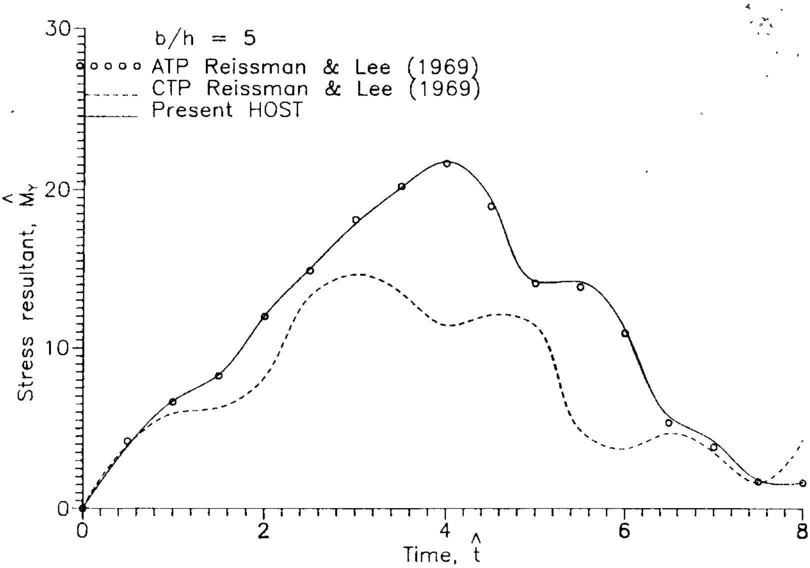

Figure 2b. *Stress resultant vs. time for a simply supported (S1), rectangular isotropic plate under suddenly applied patch load (q_o = 1, Δt = 0.02 sec).*

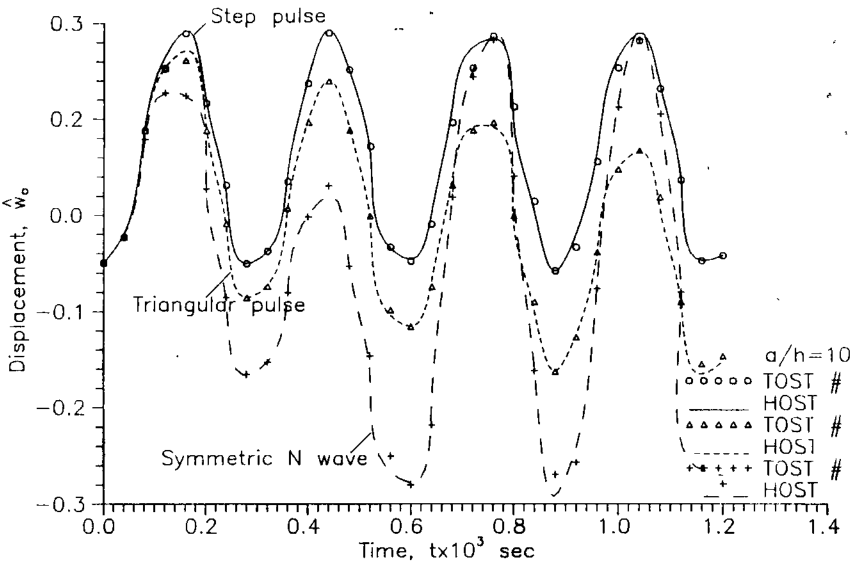

Figure 3. *Displacement vs. time for a simply supported (S1) square orthotropic three-layer plate (q_o = 4500 psi, Δt = 1 μsec).*

sponses given by Nosier and Reddy (1991) and are presented in Figure 3. The non-dimensional quantity for representing displacement is as follows:

$$\hat{w}_o = \left(\frac{w_o}{h}\right) \tag{21}$$

The present results match exactly with the closed-form third order theory solution given by Nosier and Reddy (1991).

6.2 Geometric Non-Linear Analysis

6.2.1 INFINITE LONG PLATE

A clamped (C) isotropic plate, which is infinitely extended in one direction is modelled, invoking symmetry by 5 plate bending elements. The loading is a suddenly applied, uniformly distributed, pulse load; geometry and material properties are as per material set 3. The present results are compared with Pica and Hinton (1980); they are presented in Figure 4. The present results match exactly with the Pica and Hinton (1980) results, which validates the present formulation in geometric non-linear regime.

6.2.2 SQUARE LAMINATES

A simply supported (S2) laminate of $a/h = 10$ with laminations (0°/90°) and (45°/−45°) and material properties as per material set 4 subjected to a uniform pulse load is considered. This problem is selected to compare the present results with Reddy (1983) who used an implicit time matching scheme; the results are presented in Figures 5a and 5b. The correlation is excellent. Since the laminates considered are moderately thick where the shear deformation effects are not much pronounced, the predictions of FOST and HOST are identical. This result establishes further the validity of the present non-linear formulation.

6.2.3 SANDWICH LAMINATE

A clamped (C) angle-ply (0°/45°/90°/CORE/90°/45°/30°/0°) sandwich laminate with geometry and material properties as per material set 5 subjected to a suddenly applied uniform pulse load is considered. The results are presented in Figures 6a and 6b for linear and geometrically non-linear analyses by using first order shear deformation theory, higher order shear deformation theory, and the corresponding linear analysis results of Kant (1987). Further, the behaviour of the laminate by changing the core properties is also studied. The non-dimensional quantities used are as follows:

$$\hat{w}_o = \frac{w_o}{h} \; ; \; \hat{\sigma}_x = \frac{\sigma_x}{E_2}\left(\frac{a}{h}\right)^2 \tag{22}$$

The present linear results match exactly with Kant (1987). From the results, it is confirmed that even at $a/h = 10$ first order shear deformation theory under-predicts the displacements in linear as well as geometric non-linear analyses. It

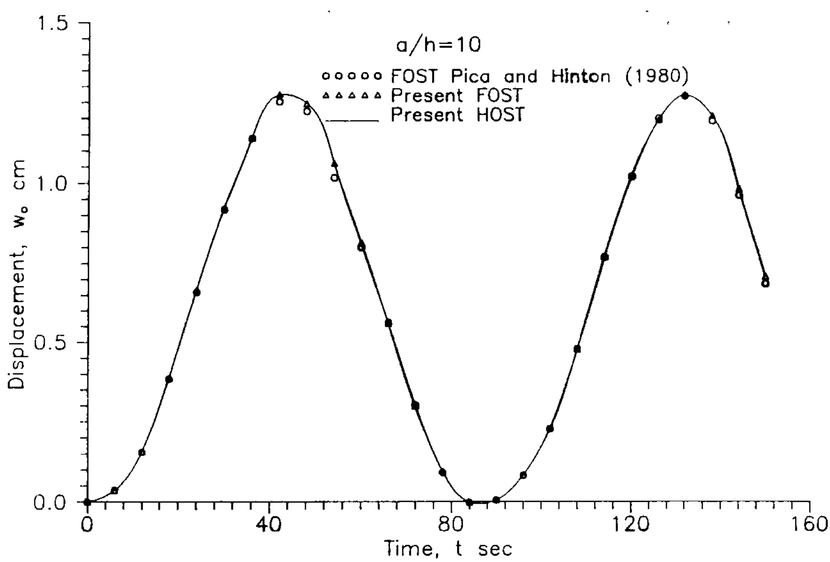

***Figure 4.** Displacement vs. time for an infinite long isotropic plate under suddenly applied uniform pulse load (q_o = 0.02 kg/cm^2, Δt = 0.06 sec).*

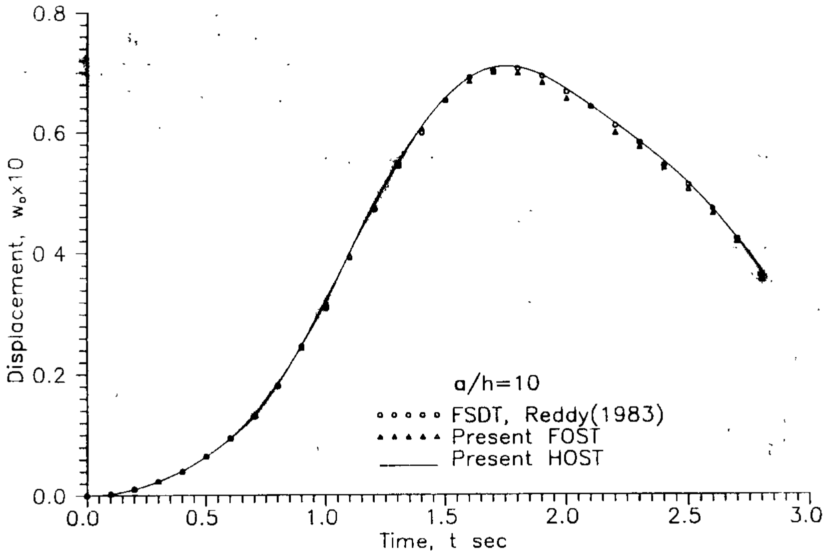

Figure 5a. *Displacement vs. time for a simply supported (S2) square cross-ply (0°/90°) laminated plate under suddenly applied uniform pulse load (q_o = 0.005, Δt = 0.01 sec).*

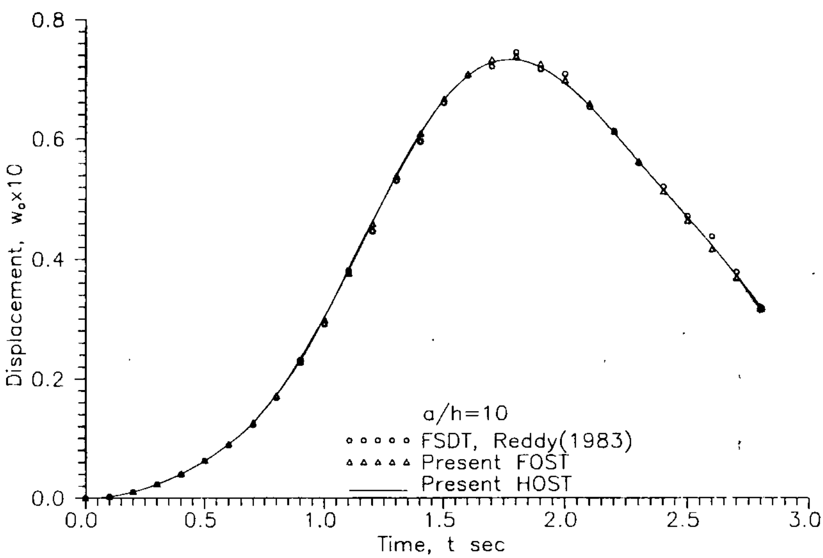

Figure 5b. *Displacement vs. time for a simply supported (S2) square angle-ply (45°/−45°) laminated plate under suddenly applied uniform pulse load (q_o = 0.005, Δt = 0.01 sec).*

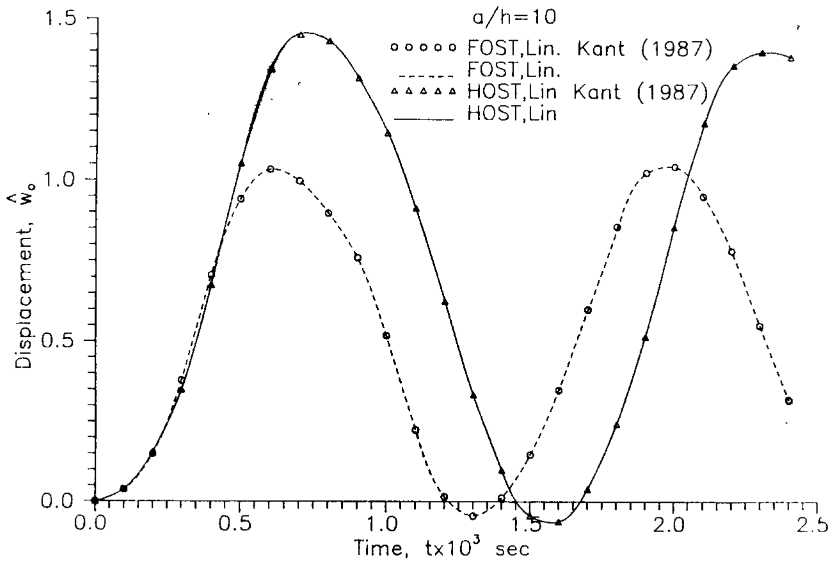

Figure 6a. *Displacement vs. time for a clamped (C) angle-ply sandwich (0°/45°/90°/CORE/90°/45°/30°/0°) laminate under suddenly applied uniform transverse load (q_o = 5000 N/cm^2, Δt = 5 μsec).*

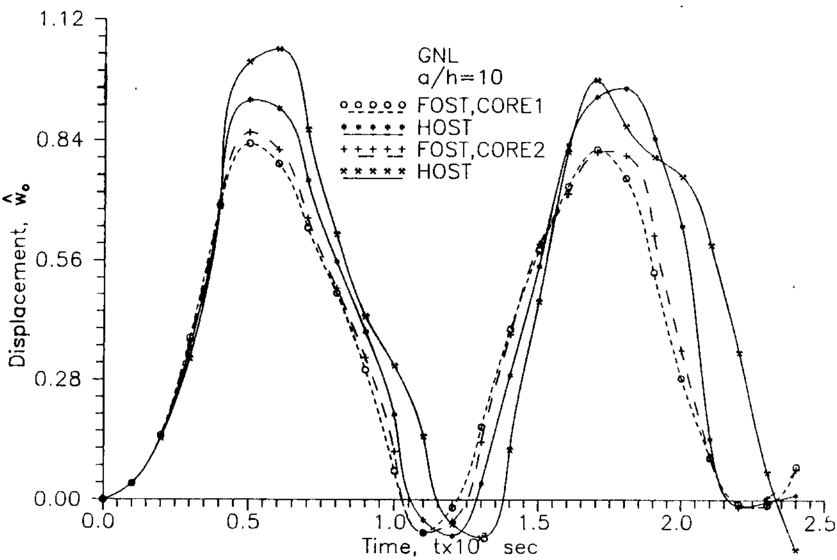

Figure 6b. *Displacement vs. time for a clamped (C) angle-ply sandwich (0°/45°/90°/CORE/90°/45°/30°/0°) laminate under suddenly applied uniform transverse load (q_o = 5000 N/cm^2, Δt = 5 μsec).*

is also to be noted that because of non-linearity the amplitude of vibration is reduced when compared with linear responses. The FOST predictions for different core properties do not differ much, but the corresponding predictions with HOST vary considerably. This result may be due to the warping of the transverse cross section, which is not possible with FOST. The usefulness of the formulation is thus evident.

6.3 Combined Geometric and Material Non-Linear Analysis

6.3.1 AN ISOTROPIC PLATE

A simply supported (S2) isotropic plate with $a/h = 20$ and material properties as per material set 6 subjected to an uniformly distributed transverse load of intensity $q_o = 300$ psi is considered. The present results, compared with Liu and Lin (1979), are plotted in Figure 7 for linear, geometric non-linear, material non-linear, and combined geometric and material non-linear analyses. It is seen that the effect of material non-linearity is softening of the plate; therefore, the amplitude of displacement is larger than the linear elastic behaviour. The present linear and material non-linear responses, compared with Liu and Lin (1979), are in good agreement. New results are also presented for combined geometric and material non-linear responses. These results are intended to serve as benchmarks for future investigations. As expected, there is not much difference between FOST and HOST predictions, which may be due to negligible shear deformation effects. Further, it is clear that the two non-linearities are of opposing type; there-

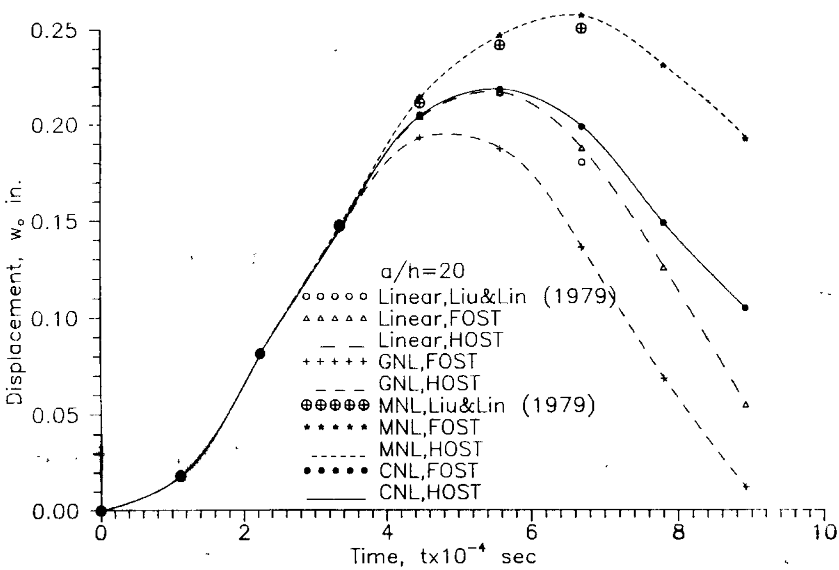

Figure 7. *Displacement vs. time for a simply supported (S2) isotropic plate under suddenly applied uniformly distributed transverse load.*

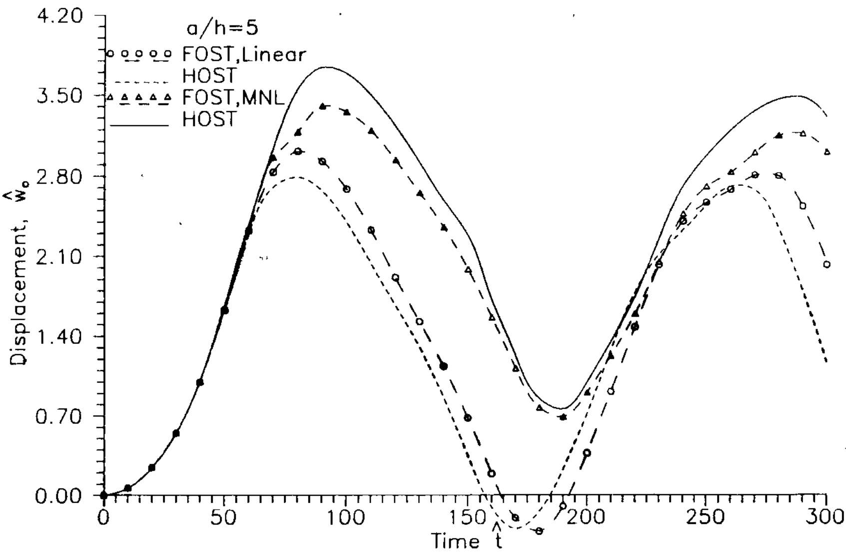

Figure 8. Displacement vs. time for a clamped (C) angle-ply (45°/−45°) laminate under suddenly applied uniformly distributed transverse load (Δt = 0.5 μsec, q_o = 0.9375).

fore, the results of combined non-linearity are closer to the linear solution. Such behaviour is incidental to, rather than typical of, all the problems.

6.3.2 AN ANGLE-PLY LAMINATE

A clamped (C) angle-ply (45°/−45°) plate with $a/h = 5$ and material properties as per material set 7 subjected to an uniformly distributed transverse load of intensity $\hat{q}_o = 0.9375$ is considered. The present linear and material non-linear responses are plotted in Figure 8 both with FOST and HOST. The laminate is a thick one. As expected there is a difference between FOST and HOST predictions up to an extent of 10%. The usefulness of the present HOST formulation may thus be seen. The following non-dimensional quantities are used to present the results:

$$\hat{q}_o = \frac{q_o}{E_2}\left(\frac{a}{h}\right)^4 ; \hat{w}_o = \left(\frac{w_o}{h}\right) \tag{23}$$

6.3.3 A CROSS-PLY LAMINATE

A simply supported (SI) cross-ply (0°/90°/0°) plate with $a/h = 40$ and the material properties as per material set 7 subjected to an uniform transverse load of intensity $\hat{q}_o = 51.2$ is considered. The present linear and non-linear responses are plotted in Figure 9 with both FOST and HOST. As expected, the predictions with both the theories are identical, which may be due to the negligible shear deformation effects as the plate considered is thin. Further, it is to be noted that the GNL displacement response is less than the corresponding linear response; however, the MNL and CNL displacement responses are larger than the linear responses. The CNL response lies in between the individual non-linear responses. The non-dimensional quantities are as per Equation (23).

7. CONCLUSIONS

Numerical results of the linear and non-linear analyses of isotropic, orthotropic, and layered composite and sandwich laminates are presented. The simple C° isoparametric formulation of an assumed higher order displacement model employed here is stable and accurate in predicting the linear and non-linear transient responses of composite and sandwich laminates. In contrast to first order shear deformation theory, the present theory does not require the usual shear correction factors generally associated with the first order shear deformation theory. The present finite element results in linear and non-linear analyses agree very well with the available analytical and other finite element solutions in the literature. The simplifying assumptions made in classical plate theory (CPT) and first order shear deformation theory (FOST) are reflected by a high percentage of errors especially in the predictions of sandwich laminates. It is believed that the refined shear deformation theory presented herein is essential for predicting accurate responses of sandwich laminates. The present results of essentially non-linear analyses of composite plates should serve as reference results for future investigations.

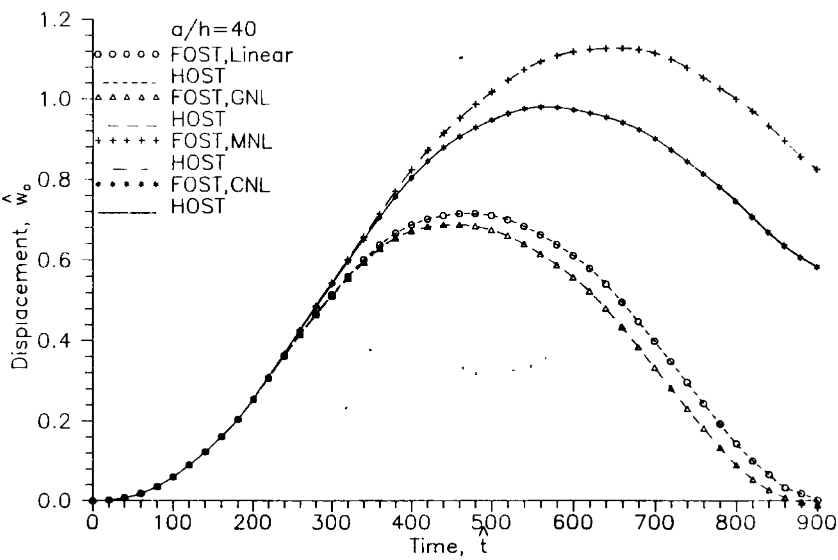

Figure 9. *Displacement vs. time for a simply supported (S1) cross-ply (0°/90°/0°) laminate under suddenly applied uniformly distributed transverse load.*

ACKNOWLEDGEMENT

The authors gratefully acknowledge partial support of this research by the Aeronautics Research and Development Board, Ministry of Defence, Government of India through its Grant Nos. Aero/RD-134/100/10/88–89/518 and Aero/RD-134/100/10/88–89/534.

REFERENCES

Hinton, E. and D. R. J. Owen. 1984. *Finite Element Software for Plates and Shells.* Swansea, UK: Pineridge Press.

Kant, T. 1987. "Transient Dynamics of Fibre Reinforced Composite Plates," Research Report, IIT-B/CE/RR/87/1, Dept. of Civil Engineering, Indian Institute of Technology, Bombay, India.

Kant, T. and J. R. Kommineni. 1992a. "Geometrically Non-Linear Analysis of Doubly Curved Laminated and Sandwich Fibre Reinforced Composite Shells with a Higher Order Theory and C° Finite Elements," *J. Reinforced Plastics and Composites,* 11:1048–1076.

Kant, T. and J. R. Kommineni. 1992b. "An Unified Large Deflection Elastics and Dynamics of Composite Laminates," *Int. Conf. Computational Mech. Engg. 1992, Singapore Nov. 11–13, 1992.*

Kant, T. and J. R. Kommineni. 1992c. "C° Finite Element Geometrically Non-Linear Analysis of Fibre Reinforced Composite and Sandwich Laminates Based on Higher Order Theory," *Comput. Struct.*, 45:511–520.

Kommineni, J. R. and T. Kant. 1993. "Pseudo-Transient Analysis of Composite Shells Including Geometric and Material Non-Linearities," *J. Reinforced Plastics and Composites,* 12:101–126.

Liu, S. C. and T. H. Lin. 1979. "Elastic-Plastic Dynamic Analysis of Structures Using Known Elastic Solutions," *Earthquake Engng. Struct. Dyn.*, 7:147–159.

Mallikarjuna and T. Kant. 1990. "Finite Element Transient Response of Composite and Sandwich Plates with a Refined Higher Order Theory," *ASME J. Appl. Mech.*, 57:1084–1086.

Nosier, A. and J. N. Reddy. 1991. "A Study of Non-Linear Dynamic Equation of Higher Order Shear Deformation Plate Theories," *Int. J. Non-Lin. Mech.*, 26:233–249.

Nanda, A. and T. Kuppusamy. 1991. "Three Dimensional Elastic-Plastic Analysis of Laminated Composite Plates," *Composite Struct.*, 17:213–225.

Owen, D. R. J. and E. Hinton. 1980. *Finite Elements in Plasticity.* West Cross, Swansea, U.K.: Pineridge Press Limited.

Pica, A. and E. Hinton. 1980. "Transient and Pseudo Transient Analysis of Mindlin Plates," *Int. J. Num. Meth. Eng.*, 15:188–208.

Reismann, H. and Y. Lee. 1969. "Forced Motions of Rectangular Plates," in *Developments in Theoretical and Applied Mechanics,* D. Frederick, editor, New York: Pergamon Press, 4:3–18.

Reddy, J. N. 1983. "Geometrically Non-Linear Transient Analysis of Laminated Composite Plates," *AIAA J.*, 21:621–629.

Tsui, T. Y. and P. Tong. 1971. "Stability of Transient Solutions of Moderately Thick Plates by Finite Difference Methods," *AIAA J.*, 9:2062–2063.